Hance, J., & Rarity, J. (2020). Counterfactual Ghost Imaging. Unpublished. https://arxiv.org/abs/2010.14292v2

Early version, also known as pre-print

Counterfactual Ghost Imaging

Jonte R. Hance[1,*] and John Rarity[1]

[1] *Quantum Engineering Technology Laboratory, Department of Electrical and Electronic Engineering, University of Bristol, Woodland Road, Bristol, BS8 1UB, UK*

(Dated: November 3, 2020)

We give a protocol for ghost imaging in a way that is always counterfactual - while imaging an object, no light interacts with that object. This extends the idea of counterfactuality beyond communication, showing how this interesting phenomenon can be leveraged for metrology. Given, in the infinite limit, no photons ever go to the imaged object, it presents a method of imaging even the most light-sensitive of objects without damaging them. Even when not in the infinite limit, it still provides a many-fold improvement in visibility and signal-to-noise ratio over previous protocols, with up to multiple orders of magnitude reduction in absorbed intensity.

INTRODUCTION

Ghost Imaging exploits the the position-momentum entanglement between correlated photon pairs to derive image information. When one photon of the pair travels via the object and is focused into a bucket detector, an image can still be formed using coincident detection of the partner photon in a high-resolution pixel detector [1–4] (as shown in Fig1). While Pittman et al originally conceived ghost imaging to illustrate the power of quantum correlations [5], it has since been shown thermal/classically-correlated light can be used to replicate this effect classically [6–9]. However, doing this, rather than using a pair of entangled photons, removes some of the benefits of the original quantum protocol. Specifically, entangled pairs of photons created in spontaneous parametric downconversion (SPDC) are both correlated in terms of position (meaning they can image in the near-field), and anti-correlated in terms of momentum, meaning they are anti-correlated in position in the far-field, so can image there too - whereas classically, they can only be (anti-)correlated in one of the two conjugate variables, so can only image in one of these regimes. Therefore, despite the comparative ease of using thermal light, it makes more sense to image using entangled photon pairs. However, despite what may have been claimed [10], using short wavelength light for the photons going to the high-resolution detector and longer wavelengths to the object does not allow an increase in imaging resolution above and beyond standard diffraction limits [11]. In any case, the ability to ghost image while reducing the energy going to the object under investigation, to reduce potential damage, could be massively beneficial.

Counterfactuality, an extension of Interaction-Free Measurement, is the idea of using quantum effects to either probe objects or send messages without any matter/energy passing between the two parties when information is transferred [12]. This is based on Elitzur and Vaidman's Interaction-Free Bomb Detector [13], where a bomb, set to trigger on detecting the presence of a single photon, is put in one of the arms of a Mach-Zehnder interferometer. Even if the bomb doesn't blow up, the field travelling (or blocked by the bomb) affects the interference pattern created at the output of the interferometer. The original protocol, using 50:50 beamsplitters, was inefficient, having a high probability of causing explosion. Since then, adaptions have been made that reduce the probability of the photon going via the bomb's path to nearly zero [14, 15]. Extending the protocol to more mundane but realistic application scenarios, Salih et al created a communication protocol based on this idea, where Alice obtains a different result depending on whether or not Bob blocks his side of a channel, without any chance of the photon having gone via Bob [16, 17] (which has even led to protocols which send quantum information

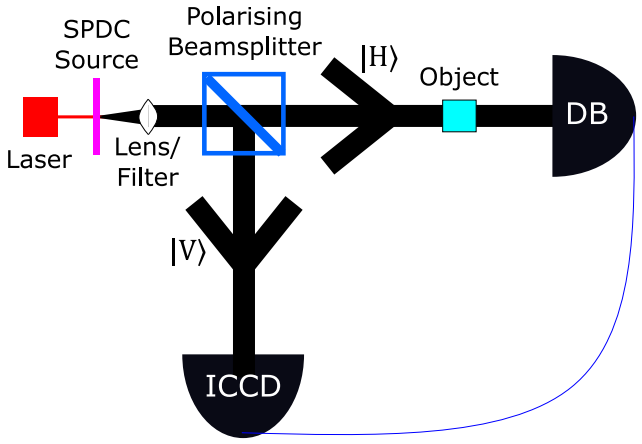

FIG. 1. A standard set-up for ghost imaging. Position-and-momentum-entangled photons are generated in pairs at the spontaneous parametric downconversion (SPDC) source from a laser beam, with conjugate polarisations (i.e. always in pairs of horizontal and vertical polarisation). A polarising beamsplitter sends the vertically polarised photon to an intensified charge-coupled device (ICCD) camera (which records in high resolution its arrival position), and sends the horizontally-polarised photon via a sample to be imaged, to a bucket detector (DB). By recording coincidences between the detections at the ICCD and the bucket detector, the sample can be "ghost imaged".

counterfactually [18–21]). Given, in this protocol, the photon provably never travels via Bob when information is transmitted [22], it raises the question of whether this protocol could be adapted to probe an object counterfactually.

Zhang et al combined Ghost Imaging with the Elitzur-Vaidman Bomb Detector [13] to create a form of Ghost Imaging where there is a chance that information is still received about the imaged object without any photons being absorbed by it [23]. However, the Elitzur-Vaidman Bomb Detector is not always necessarily counterfactual - there is a (reasonably high) chance the photon can go via the object being investigated [12]. By replacing the Elitzur-Vaidman object-detection system in Zhang's protocol with Salih et al's method for counterfactual communication, we create a protocol for ghost imaging that is always counterfactual - whenever information is received about the imaged object, no photons have interacted with that object.

Further, even in cases when no information travels, far fewer photons go to the object than in either the standard ghost imaging or in the interaction-free ghost imaging case - reducing the energy absorbed by the object, and so potentially damage done to that object by the imaging process.

PROTOCOL

We first go through Salih et al's protocol for counterfactual communication, before showing how this can be adapted and integrated into Zhang et al's Interaction Free Ghost Imaging protocol.

Note, we define our polarisation Bloch sphere with poles $|H\rangle$ and $|V\rangle$, and rotation

$$\hat{\mathbf{R}}_y(\theta) = \begin{pmatrix} \cos\left(\frac{\theta}{2}\right) & -\sin\left(\frac{\theta}{2}\right) \\ \sin\left(\frac{\theta}{2}\right) & \cos\left(\frac{\theta}{2}\right) \end{pmatrix} = e^{-i\theta\hat{\sigma}_y/2} \tag{1}$$

for dummy variable θ (in terms of Pauli-y operator $\hat{\sigma}_y$).

A photon of state $a\,|H\rangle + b\,|V\rangle$ enters the outer interferometer through a Half Wave Plate (HWP), tuned to apply $\hat{\mathbf{R}}_y(\pi/M)$. It then enters a Polarising Beam Splitter (PBS), which transmits horizontal polarisation, but reflects vertical.

The vertical element then passes through a chain of N inner interferometers. In these it goes through a HWP tuned to apply $\hat{\mathbf{R}}_y(\pi/N)$, then through another PBS. The newly-horizontal component passes across the channel, from Alice to Bob, who can choose to block or not block this channel (by switching on or off his switchable mirror). If he blocks, it is absorbed and lost - if not, it returns to Alice's side, recombines at another PBS with the vertical component, then enters the next inner interferometer. This happens N times. The wave is then passed through one final PBS, to remove any horizontal components, before being recombined at another PBS with the horizontal arm of the outer interferometer.

As each inner interferometer applies $\hat{\mathbf{R}}_y(\pi/N)$, if Bob doesn't block, the rotations sum to

$$\hat{\mathbf{U}}_{NB}^{N} = (e^{-i\pi\hat{\sigma}_y/2N})^N = e^{-i\pi\hat{\sigma}_y/2} = \hat{\mathbf{R}}_y(\pi) \tag{2}$$

and so the state after the inner interferometer chain is

$$|V\rangle_I \rightarrow \hat{\mathbf{U}}_{NB}^{N}\,|V\rangle_I = |H\rangle_I \rightarrow Loss \tag{3}$$

The vertical component becomes horizontally-polarised, and is lost to the final PBS. Therefore, the only element of the wavefunction leaving the outer interferometer is that which travelled the outer arm.

Similarly, if Bob blocks for all inner interferometers, because of the quantum Zeno effect,

$$\begin{aligned} \hat{\mathbf{A}}_B^{N} &= \left[e^{-i\pi\hat{\sigma}_y/2N} \begin{pmatrix} 1 & 0 \\ 0 & 0 \end{pmatrix} \right]^N \\ &= \begin{pmatrix} \cos\left(\frac{\pi}{2N}\right)^N & 0 \\ \cos\left(\frac{\pi}{2N}\right)^{N-1} \sin\left(\frac{\pi}{2N}\right) & 0 \end{pmatrix} \end{aligned} \tag{4}$$

where $\hat{\mathbf{A}}_B^{N}$ is non-unitary. Therefore, the state after the outer interferometer is

$$\begin{aligned} |V\rangle_I \rightarrow & \hat{\mathbf{A}}_B^{N}\,|V\rangle_I \\ &= \cos\left(\frac{\pi}{2N}\right)^N |V\rangle_I + \cos\left(\frac{\pi}{2N}\right)^{N-1} \sin\left(\frac{\pi}{2N}\right) |H\rangle_I \\ &\rightarrow \cos\left(\frac{\pi}{2N}\right)^N |V\rangle + Loss \end{aligned} \tag{5}$$

so some vertically-polarised component exits the outer interferometer.

This means the outer cycle applies

$$\begin{pmatrix} 1 & 0 \\ 0 & 0 \end{pmatrix} e^{-i\pi\hat{\sigma}_y/2M} \tag{6}$$

if Bob doesn't block, or

$$\begin{pmatrix} 1 & 0 \\ 0 & \cos\left(\frac{\pi}{2N}\right)^N \end{pmatrix} e^{-i\pi\hat{\sigma}_y/2M} \tag{7}$$

if he does. They repeat this M times, starting with a horizontally-polarised photon, and using a final PBS to split it into horizontal and vertical components.

Because Alice applies $\hat{\mathbf{R}}_y(\pi/M)$ at the start of each outer interferometer, if Bob doesn't block, the state of the photon after M outer cycles is

$$\cos\left(\frac{\pi}{2M}\right)^M |H\rangle \tag{8}$$

meaning, if it isn't lost, it remains horizontally-polarised (and goes into D_0). However, if he blocks, the state of

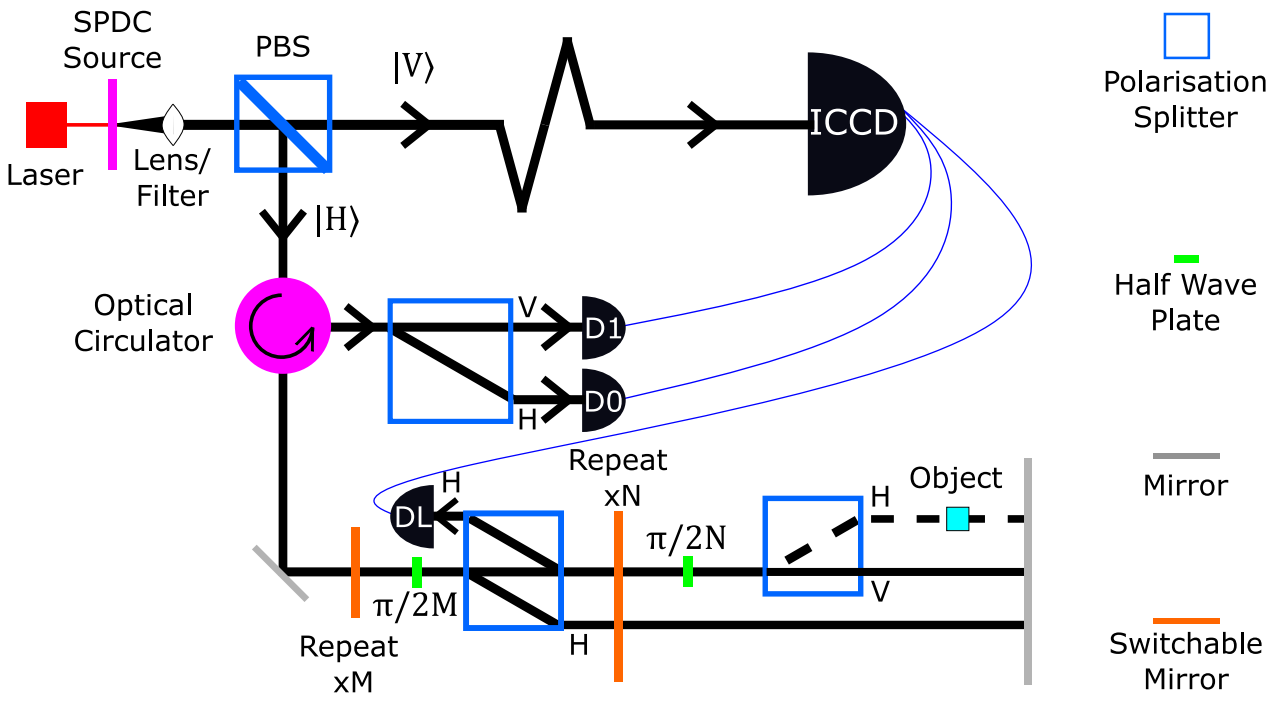

FIG. 2. Our Counterfactual Ghost Imaging Protocol, based on the combination of standard Ghost Imaging (Fig1) and a common-path interferometer version of Salih et al's counterfactual communication protocol [16]. We create a pair of position-and-momentum-entangled photons, one horizontally polarised and one vertically polarised, by passing a pulsed pump laser through a spontaneous parametric downconversion (SPDC) crystal, before collimating the beam, and filtering out the pump. The photon pair is split at a polarising beamsplitter (PBS), with the V-polarised photon going through a long optical delay to an Intensified Charge-Coupled Device (ICCD) camera, and the H-polarised photon going through a run of Salih et al's protocol, adapted so the object to be investigated is put in place of Bob's blocker. The switchable mirrors allow the photon to cycle the correct number of times: the first for M outer cycles; and the second for N inner cycles per outer cycle. The polarisation separators subtly divert horizontally-polarised light, and directly transmit vertically-polarised light. The Half Wave Plates are tuned to implement a $\hat{\mathbf{R}}_y(\theta)$ polarisation-mode rotation with θ of $\pi/2M$ and $\pi/2N$ respectively. The detector D_L acts as our loss channels (which we postselect against). After M outer cycles, the switchable mirror sends the photon to the optical circulator, which sends it to the PBS. The path not being blocked by the object leads the photon to remain H-polarised, and so go to $D0$, leading to a coincidence measurement between that and the ICCD camera; however, the path being blocked leads to the photon becoming V-polarised and so going to $D1$, so coincidence measurement between that and the ICCD. The use of multi-mode interferometers and (position-momentum) correlations between the entangled photons enables multi-mode ghost imaging in this counterfactual set-up. Note, the polarisation separators ensure a common path length for both $H-$ and V-polarised components, while generating beam separations of the several millimetres. An optimisation we mention in the discussion has photons going to DL can trigger a coincidence measurement with the ICCD, treated as if it was a detection at $D0$, which does not affect the chance of photons interacting with the object (photons only go to DL if the object doesn't block the channel), and allows us to lower the number of outer cycles to the minimum required (2) with no increase in loss.

the photon after M outer cycles (as $N \to \infty$) is $|V\rangle$, and it becomes vertically polarised (and goes into D_1).

We now describe how to adapt the above protocol to use it for Counterfactual Ghost Imaging (as shown in Fig.2). A pair of conjugately-polarised photons, entangled in position and momentum, are split at a polarising beamsplitter, with the vertically-polarised one going through an image-preserving optical delay line to an Intensified Charge-Coupled Device (ICCD) camera (both of which have previously been used to allow multi-mode, rather than single-mode raster-scanning, ghost imaging [3, 10, 24]), and the horizontally-polarised one going through one run of Salih et al's protocol, where the object to be imaged is put in place of Bob's blocker. The path not being blocked by the object leads the photon, in that spatial mode to remain horizontally-polarised, and so go to $D0$, leading to a coincidence measurement between $D0$ and that pixel of the ICCD camera; however, the path being blocked leads to the photon becoming V-polarised and so going to $D1$, and a coincidence measurement between $D1$ and that pixel of the ICCD camera.

Note, because arrival in $D0$ ($D1$) is correlated far more closely (see Fig.3b) in Salih et al's protocol with the object not blocking (blocking) the path than in the Elitzur-Vaidman Bomb Detector (and so Zhang et al's protocol [23]), we only **need** to resolve coincidences between $D0$

and the ICCD (unlike Zhang et al, who need to form two images - one based on $D0$-ICCD coincidences, and the other on $D1$-ICCD coincidences - and subtract one from the other, due to the interference patterns produced by the Elitzur-Vaidman Bomb Detector [13]). However, by resolving both $D0$-ICCD and $D1$-ICCD coincidences, and subtracting one from the other, we can image with high accuracy even for low N - so we do this.

Note, a similar protocol can be constructed by replacing Salih et al's protocol in the imaging set-up with either Aharonov and Vaidman's modified protocol [25], or Vaidman's later adaptation [26] - however, such a protocol would not be counterfactual by the Consistent Histories criterion (as shown by Salih [19, 22]).

For the original Ghost Imaging protocol, photon pairs are generated by spontaneous parametric down-conversion (SPDC) [5]. This makes use of second-order nonlinearities in an optical medium to generate conjugately-polarised photon pairs entangled in position and with frequencies that sum to the frequency of an input pump laser. By using a low-pass filters, the photons can be split off from the pump laser, and then split from one another using a polarising beamsplitter, sending one to the high-resolution detector, and the other to the object and bucket detector. We propose using exactly the same source for our protocol.

Also note, for the V-polarised photon going to the ICCD, rather than using an optical delay, the ICCD can detect the photon earlier, but record the time of arrival as well as the position, which can be used with post-processing to determine coincidences (if path length was equal) with the bucket detectors, avoiding issues with long optical delays.

DISCUSSION

When considered from the perspective of communication, Salih et al's protocol is fully counterfactual - when Alice detects her photon in either $D0$ or $D1$, she can be sure it has never been to Bob. However, when the number of cycles isn't infinite, there is a chance the photon could go via Bob, in which case the protocol is aborted and restarted. Given a use of Ghost Imaging is to image photosensitive samples (which could be easily damaged by high-energy photons), we want to reduce the chance of any photons going to/via the object as much as possible. We plot this probability in Fig.3a. Note, as N goes to infinity, this probability goes to zero.

In Salih et al's 2013 protocol, there is a probability of erroneous $D0$ clicks, as they take $\cos(\pi/2N)^N \to 1$ for large N. This probability, for $M = 2$, is

$$P(D0|Block)_{M=2} = \left(\cos\left(\frac{\pi}{2N}\right)^N - 1\right)^2/4 \qquad (9)$$

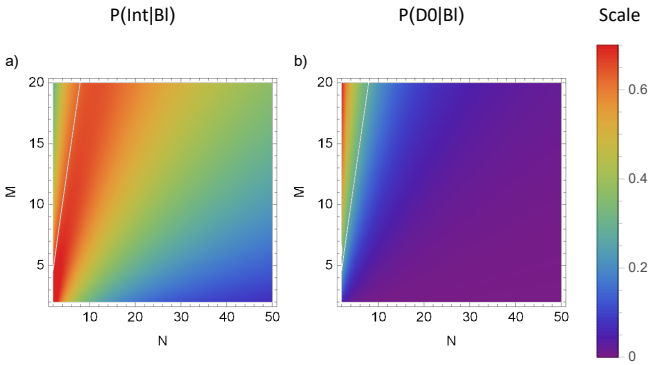

FIG. 3. Probability, when the object blocks the channel, of the photon: interacting with the object being imaged (P_{Int}) (a); or erroneously ending up in $D0$ (b). We plot these for given numbers of outer (M) and inner (N) interferometer cycles. Note, the photon only goes via the object erroneously - in any case when $D1$ clicks, the detection of the object will have been fully counterfactual. Further, both the interaction and erroneous-$D0$ probabilities go to 0 as N goes to ∞.

We plot the probability for given values of M and N in Fig.3b. By increasing the rotation slightly at the start of each outer cycle, this error could be avoided - future work will consider the exact value needed, and the specific benefits of this optimisation.

The signal-to-noise ratio (SNR) [27–29], a useful measure of the efficacy of an imaging system, is given by

$$\text{SNR} = \frac{|\Delta\bar{I}|}{\sigma(|\Delta\bar{I}|)} \qquad (10)$$

where $\Delta\bar{I}$ is the difference in average intensity values observed by a detector between inside and outside the object, and $\sigma(|\Delta\bar{I}|)$ is the standard deviation in this difference.

For standard ghost imaging, when an average of $\bar{N}$ photons (those generated in a given time interval by a SPDC source) interrogate an object, none of the $\bar{N}$ photons will reach the detector, giving a change in photon detection number at the detector of $\Delta N_{GI} = -\bar{N}$. Given spontaneous parametric down-conversion has thermal statistics for rate of emission, which look Poissonian as it is averaged over many temporal modes, this means the signal to noise ratio (SNR) is

$$\text{SNR}_{GI} = \bar{N}/\sqrt{\bar{N}} = \sqrt{\bar{N}} \qquad (11)$$

For counterfactual ghost imaging, we define ΔN_{D0} (ΔN_{D1}) as the difference in photon numbers received at $D0$ ($D1$) between the object blocking and not blocking the channel (which in each case is $\bar{N}$ times the difference in probability of a photon reaching that detector in each of those two cases). Note, ΔN_{D0} and ΔN_{D1} will have

opposite signs. Therefore,

$$\begin{aligned}\mathrm{SNR}_{CGI} &= \frac{|\Delta N_{D0} - \Delta N_{D1}|}{\sigma(|\Delta N_{D0} - \Delta N_{D1}|)} \\ &= f(M,N)\sqrt{\bar{N}} = f(M,N)\mathrm{SNR}_{GI}\end{aligned} \tag{12}$$

which we plot in Fig.4a (as a multiple of SNR_{GI}, the SNR of standard ghost imaging). For values of M and N where $\mathrm{SNR}_{CGI} = 1$, the protocol is just as good at imaging as standard ghost imaging. In these cases, Fig.3b shows that in our protocol the probability of a photon interacting with the object is much less than the 73.5% limit from previous protocols [23].

However, rather than looking at the SNR for the photons generated by a SPDC source in a given period of time, a more apt comparison would be the SNR for which the same number of photons are absorbed by the object as in standard ghost imaging. Given the average number of photons interacting with the object is P_{Int} times $\bar{N}$, we get

$$\mathrm{SNR}_{Int} = f(M,N)\sqrt{\bar{N}/P_{Int}} = \frac{f(M,N)}{\sqrt{P_{Int}}}\mathrm{SNR}_{GI} \tag{13}$$

which we plot in Fig.4b (again in terms of SNR_{GI}).

Even for low numbers of outer and inner cycles (M and N), our protocol gives a vast improvement over the signal-to-noise ratio of standard ghost imaging - for instance, two outer cycles of 13 inner cycles gives double the equal-photon-absorption SNR of standard ghost imaging. Note, as $N \to \infty$, the probability of a photon interacting with the object goes to 0, meaning SNR_{Int} becomes infinitely larger than the SNR available with standard ghost imaging (if we're willing to wait that long).

Another key measure of an imaging protocol's efficacy is its visibility, V, defined as

$$V = \frac{|\bar{N}_{In} - \bar{N}_{Out}|}{\bar{N}_{In} + \bar{N}_{Out}} \tag{14}$$

Visibility gives how responsive to a difference in presence/absence of an object is, defined on a scale from 0 to 1. For our protocol, visibility is given as

$$V_{CGI} = \frac{|\Delta N_{D0} - \Delta N_{D1}|}{2\bar{N}} \tag{15}$$

(the changes in intensity for $D0$ and $D1$ over the maximal possible changes in their intensities, remembering their opposite signs). This gives reasonable values (i.e. between 0 and 1) for our protocol, as given in Fig.4c - for instance, 5 outer cycles of 12 inner cycles gives a visibility of 0.569.

When the object does not block the photon's path in the adapted Salih et al device, for finite numbers of outer interferometers (M), there is a chance the photon will cross through the unblocked gap, in which case it goes to the loss detector DL rather than the coincidence-linked detector $D0$. This occurs with probability

$$P(DL|NB) = 1 - \cos\left(\frac{\pi}{2M}\right) \tag{16}$$

which we plot in Fig.5. This goes to 0 as M goes to infinity. Note, if we weaken our definition of counterfactuality to be that the photon never goes via the object's path when the object is there (rather than the photon never goes via that path at all), we could link detector DL as well as $D0$ to the ICCD, treating coincidences between DL and the ICCD as if they were between $D0$ and the ICCD. This would let us use the minimum number of outer cycles the protocol works for, two, rather than requiring higher values of M to avoid us erroneously ignoring ICCD detections. We do a version of this in Fig.2, having photons which would go to DL treated as if going to $D0$.

This led us to plot altered values for SNRs and visibility, taking into account DL now going to $D0$. These are plotted in Fig.4 (d, e and f), and give even better values for all three measures.

Traditional ghost imaging can only distinguish between whether or not a photon could have passed through a given region (i.e. whether, at that point, a mask would transmit that photon, or whether it would absorb/reflect it). This makes this style of ghost imaging bad for imaging transparent/translucent objects - which is unfortunate, given the many applications for the detection of low-contrast objects. However, Abouraddy et al, and later Gong et al, proposed [30, 31] (and Zhang et al experimentally demonstrated [32]) schemes which make use of phase-sensitivity to allow materials to be detected which, while translucent, create a change to the phase/polarisation of transmitted light. Zhang et al's interaction-free ghost imaging also demonstrated this sensitivity [23]. Further, given it relies on interference to direct the photon to one of two bucket detectors, our scheme is also sensitive to changes in phase induced by transparent objects - presenting yet another benefit of our protocol over standard ghost imaging.

CONCLUSION

We have given a protocol for ghost imaging in a way that is always counterfactual - while imaging the object, no light interacts with that object. This extends the idea of counterfactuality beyond communication, showing how this interesting phenomenon can be used for metrology. Given, in the infinite limit, no photons ever go to the imaged object, it presents a method of imaging even the most light-sensitive of objects without damaging them.

We thank Hatim Salih, Alex McMillan and Will McCutcheon for useful discussions. This work was supported by the University of York's EPSRC DTP grant

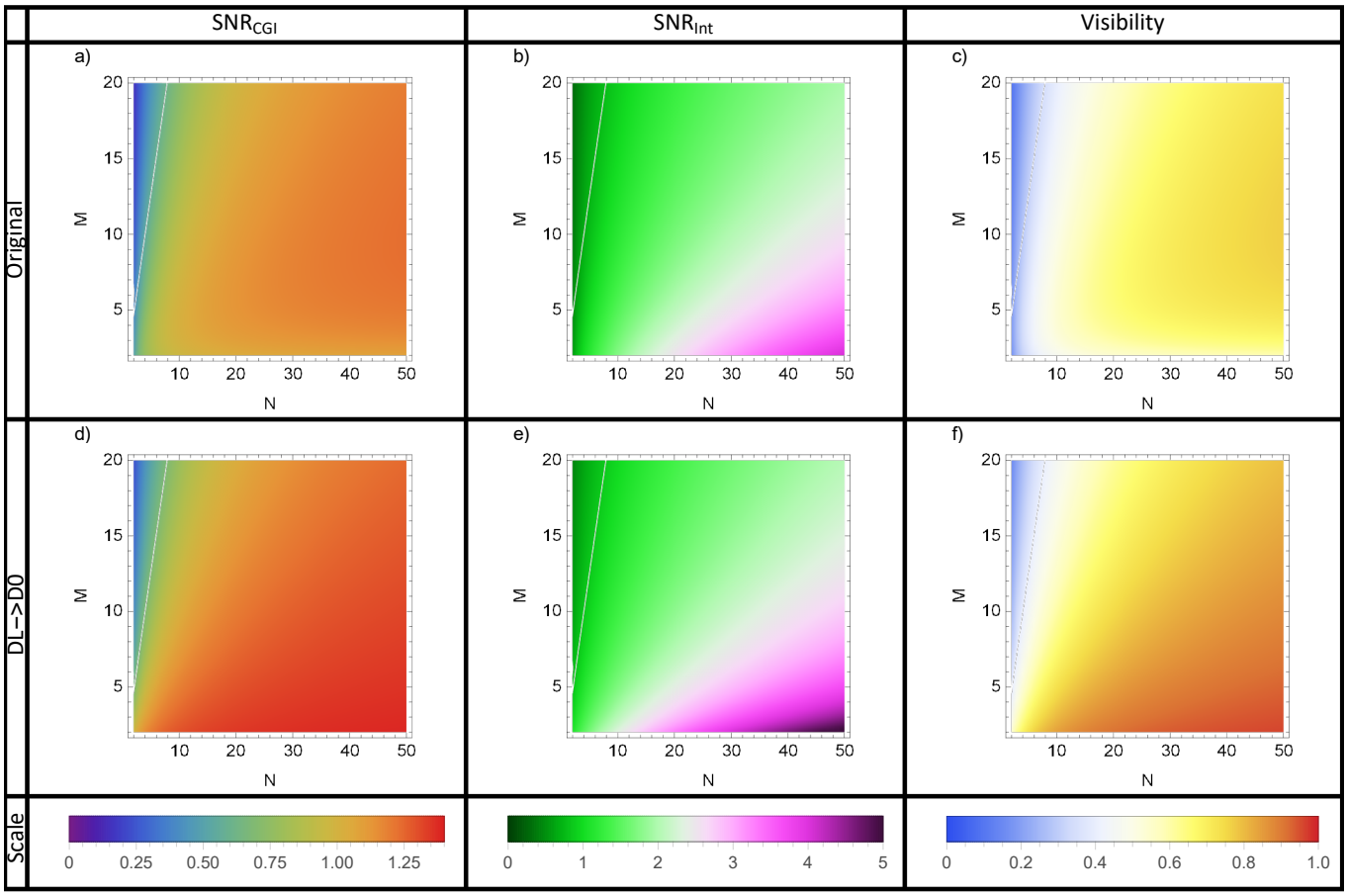

FIG. 4. Plots of the Signal-to-Noise ratio (SNR) for: equal numbers of photon pairs generated in a given time by the SPDC source (a); and equal numbers of photons absorbed by the object (b) - and the visibility V of the protocol (c) - for our original protocol; and these values for when photons that would go to DL also count for coincidence measurements as if they went to $D0$ (d,e and f). These are as functions of the number of outer (M) and inner (N) interferometer cycles.

EP/R513386/1, and the Quantum Communications Hub funded by the EPSRC grant EP/M013472/1.

* jonte.hance@bristol.ac.uk

[1] M. Malik, H. Shin, M. O'Sullivan, P. Zerom, and R. W. Boyd, Physical review letters **104**, 163602 (2010).
[2] J. H. Shapiro and R. W. Boyd, Quantum Information Processing **11**, 949 (2012).
[3] R. S. Aspden, D. S. Tasca, R. W. Boyd, and M. J. Padgett, New Journal of Physics **15**, 073032 (2013).
[4] M. J. Padgett and R. W. Boyd, Philosophical Transactions of the Royal Society A: Mathematical, Physical and Engineering Sciences **375**, 20160233 (2017).
[5] T. Pittman, Y. Shih, D. Strekalov, and A. V. Sergienko, Physical Review A **52**, R3429 (1995).
[6] R. S. Bennink, S. J. Bentley, and R. W. Boyd, Phys. Rev. Lett. **89**, 113601 (2002).
[7] Y. Cai and S.-Y. Zhu, Phys. Rev. E **71**, 056607 (2005).
[8] F. Ferri, D. Magatti, A. Gatti, M. Bache, E. Brambilla, and L. A. Lugiato, Phys. Rev. Lett. **94**, 183602 (2005).
[9] D. Duan, S. Du, and Y. Xia, Phys. Rev. A **88**, 053842 (2013).
[10] R. S. Aspden, N. R. Gemmell, P. A. Morris, D. S. Tasca, L. Mertens, M. G. Tanner, R. A. Kirkwood, A. Ruggeri, A. Tosi, R. W. Boyd, G. S. Buller, R. H. Hadfield, and M. J. Padgett, Optica **2**, 1049 (2015).
[11] P.-A. Moreau, E. Toninelli, P. A. Morris, R. S. Aspden, T. Gregory, G. Spalding, R. W. Boyd, and M. J. Padgett, Opt. Express **26**, 7528 (2018).
[12] J. R. Hance, J. Ladyman, and J. Rarity, arXiv preprint arXiv:1909.07530 (2019).
[13] A. C. Elitzur and L. Vaidman, Foundations of Physics **23**, 987 (1993).
[14] P. Kwiat, H. Weinfurter, T. Herzog, A. Zeilinger, and M. A. Kasevich, Phys. Rev. Lett. **74**, 4763 (1995).
[15] A. G. White, J. R. Mitchell, O. Nairz, and P. G. Kwiat, Phys. Rev. A **58**, 605 (1998).
[16] H. Salih, Z.-H. Li, M. Al-Amri, and M. S. Zubairy, Phys. Rev. Lett. **110**, 170502 (2013).
[17] Y. Cao, Y.-H. Li, Z. Cao, J. Yin, Y.-A. Chen, H.-L. Yin, T.-Y. Chen, X. Ma, C.-Z. Peng, and J.-W. Pan, Proceedings of the National Academy of Sciences 10.1073/pnas.1614560114 (2017).

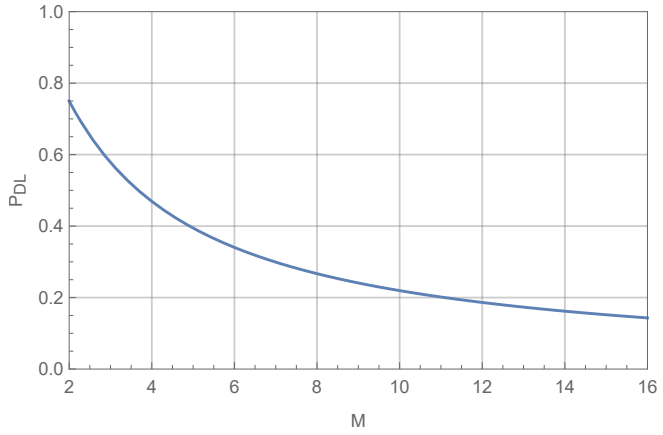

FIG. 5. Probability that, when the object does not block the photon's path, the photon travels via that path (and so goes to DL rather than $D0$). This is as a function of number of outer cycles (M).

[18] H. Salih, arXiv preprint arXiv:1404.2200v1 (2014); Frontiers in Physics **3**, 94 (2016).
[19] H. Salih, arXiv preprint arXiv:1807.06586 (2018).
[20] H. Salih, J. R. Hance, W. McCutcheon, T. Rudolph, and J. Rarity, arXiv preprint arXiv:2008.00841 (2020).
[21] H. Salih, J. R. Hance, W. McCutcheon, T. Rudolph, and J. Rarity, arXiv preprint arXiv:2009.05564 (2020).
[22] H. Salih, W. McCutcheon, J. R. Hance, and J. Rarity, arXiv preprint arXiv:1806.01257 (2018).
[23] Y. Zhang, A. Sit, F. Bouchard, H. Larocque, F. Grenapin, E. Cohen, A. C. Elitzur, J. L. Harden, R. W. Boyd, and E. Karimi, Optics Express **27**, 2212 (2019).
[24] P. A. Morris, R. S. Aspden, J. E. Bell, R. W. Boyd, and M. J. Padgett, Nature communications **6**, 1 (2015).
[25] Y. Aharonov and L. Vaidman, Phys. Rev. A **99**, 010103(R) (2019).
[26] L. Vaidman, Physical Review A **99**, 052127 (2019).
[27] M. N. O'Sullivan, K. W. C. Chan, and R. W. Boyd, Phys. Rev. A **82**, 053803 (2010).
[28] G. Brida, M. V. Chekhova, G. A. Fornaro, M. Genovese, E. D. Lopaeva, and I. R. Berchera, Phys. Rev. A **83**, 063807 (2011).
[29] M. Genovese, Journal of Optics **18**, 073002 (2016).
[30] A. F. Abouraddy, P. R. Stone, A. V. Sergienko, B. E. A. Saleh, and M. C. Teich, Phys. Rev. Lett. **93**, 213903 (2004).
[31] W. Gong and S. Han, Phys. Rev. A **82**, 023828 (2010).
[32] D.-J. Zhang, Q. Tang, T.-F. Wu, H.-C. Qiu, D.-Q. Xu, H.-G. Li, H.-B. Wang, J. Xiong, and K. Wang, Applied Physics Letters **104**, 121113 (2014).

Appendix: Counterfactual Computational Ghost Imaging

Alongside standard ghost imaging, which makes use of entangled photons, alternative forms have been created which instead just use classical correlations. Given this is classically simulable, a version has been demonstrated which is referred to as computational ghost imaging - where rather than sending a correlated photon to a high-resolution/scanning detector, a spatial light modulator (SLM) applies an effective reference pattern to the photon probing the object. Given counterfactual ghost imaging allows us to image an object counterfactually while preserving quantum correlations between the signal and idler photons, it can clearly preserve the classical correlations necessary for computational ghost imaging.

In such a set-up, we replace the SPDC, beamsplitter and ICCD camera with a single photon source, a spatial light modulator (SLM), a pseudo-random illumination pattern, and computational analysis. While it remains to be seen the effect the loss of quantum correlations would have on fidelity, loss, SNR and visibility, this shows the flexibility of counterfactual alterations to ghost imaging.

Modelling Realistic Component Loss

The analysis presented above assumes ideal components. Sadly, no component is ideal. In our protocol, the four key components which could through loss affect the protocol are the half-wave plates, the polarising beamsplitters, the switchable mirrors, and the detectors. In this appendix, we model the protocol with these at experimentally realistic values, to show that, even with these limitations considered, the protocol still provides a significant advantage over both standard ghost imaging, and classical metrology.

At designed-for wavelengths, half-wave plates can achieve loss (through reflection) of $\mathcal{O}(0.1\%)$; polarising beamsplitters can achieve loss (through absorption) of less than 1%, and a typical heralding efficiency for a SPDC/SPAD set-up like ours is 18%. Practically, switchable mirrors pose an issue (given typical switching times for these are of $\mathcal{O}(10^{-6}s)$, while the switching we need has to be of $\mathcal{O}(10^{-9}s)$). However, Cao et al showed how to adapt the protocol to use fixed components that alter a degree of freedom on the photon to effectively 'count' the number of cycles it has travelled, and transmit it after the right number [17]. An issue with this is lossiness (adding loss in their demonstration of 15/16 per outer cycle). Despite this, as we show in Fig.6 (which shows the same quantities as in Fig.4 albeit adjusted to take into account these losses), the SNR per photon absorbed is still far higher than for standard ghost imaging.

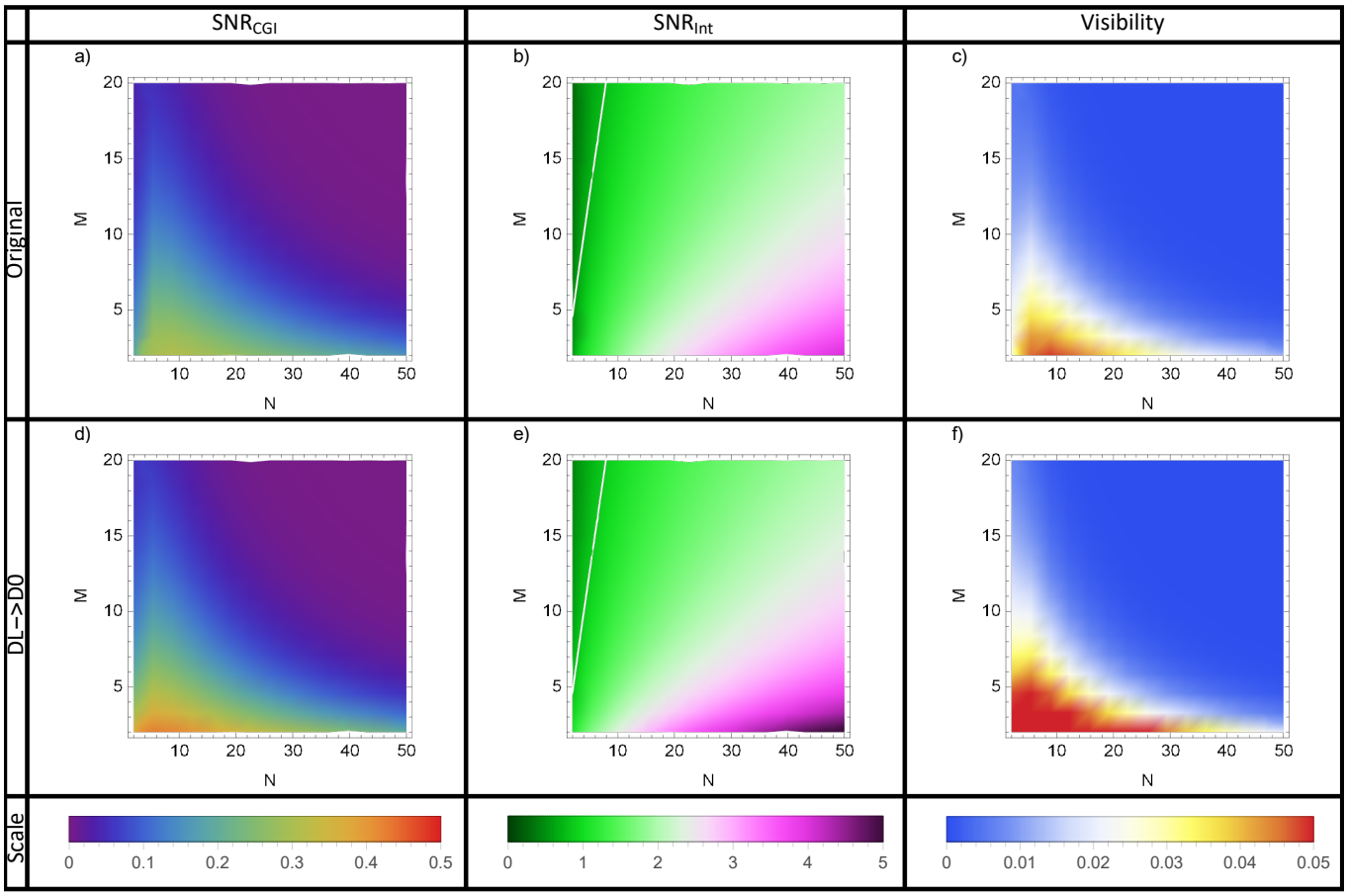

FIG. 6. SNR, SNR per photon absorbed by the sample, and visibility, for our protocol, with realistic component losses (as given in the Appendix).